Serial FDG-PET/MR Imaging for Head and Neck Cancer Radiation Therapy: A Pilot Study

Sharmili Roy, Dennis Lai-Hong Cheong, Jianhua Yan, John J. Totman, Thian Ng, Lih Kin Khor, Julian Goh and Ivan WK Tham

***Abstract*—Radiation therapy (RT), with or without chemotherapy, can be an effective organ-preserving treatment strategy for many patients with head and neck cancer. Loco-regional failure, however, can occur in a significant minority of patients. Typically, treatment response is assessed months after radiotherapy to allow the tumor to regress and to avoid confounding acute therapy effects. This paper investigates the use of hybrid 18-Flurodeoxyglucose (^{18}F-FDG) positron emission tomography/ magnetic resonance (PET/MR) imaging for early visualization of tumor changes during treatment. Qualitative and quantitative comparison of changes in the anatomical and functional parameters is presented by multi-point serial scanning of head and neck cancer patients undergoing RT. Parameters derived from diffusion weighted imaging and PET imaging are found to trend differently in the patient with recurrence in comparison to patients without recurrence. By reporting feasibility and early findings of PET/MR within treatment, this study suggests that PET/MR has the potential to demonstrate mid-treatment tumor changes. A combination of anatomical and functional parameters can be used to guide potential treatment re-planning for patients who do not respond well to the initially planned treatment strategy.**

***Index Terms*—Cancer therapy response, multi-parametric PET/MR imaging, head and neck cancer.**

I. Introduction

THE standard organ-preserving treatment strategy for the management of patients with head and neck carcinoma is radiation therapy (RT) with or without chemotherapy [1]. Tumor location, invasion of adjacent structures and presence of distant metastasis are the key factors that drive the choice of therapy [2]. Typically, a standard dose of radiation is prescribed following strict dose and volume constraints. These constraints are based on anticipated tolerance to radiation in the population instead of an individual's normal organ/or tumor radio-sensitivity. In addition, treatment response is typically assessed $3-4$ months after RT is completed to allow the acute radiation-related inflammation to resolve and to allow continued tumor cell death and apoptosis. This delayed evaluation, however, precludes the possibility of treatment re-planning for poor responders.

This research work is partially funded by the NMRC NUHS Centre Grant - Medical Image Analysis Core (NMRC/CG/013/2013).

S. Roy, D. L.-H. Cheong, J. Yan, J. J. Totman and T. Ng are with A*Star-NUS Clinical Imaging Research Centre, Singapore 117599 e-mail: (sharmili@nuhs.edu.sg, cheong_lai_hong@circ.astar.edu.sg, jianhua.yan@gmail.com, john_totman@circ.astar.edu.sg, dnrntc@nus.edu.sg).

L. K. Khor and I. W. K. Tham are with National University Health System, Singapore 119074 email:(lin_kin_khor@nuhs.edu.sg, ivan_wk_tham@nuhs.edu.sg).

J. Goh is with Tan Tock Seng Hospital, Singapore 308433 email:(julian_goh@ttsh.com.sg).

There are many clinical and pathological factors aside from primary tumor site and American Joint Committee on Cancer's tumor, nodes, metastasis (AJCC TNM) staging that influence an individual tumor's response to radiation. Some of these include metabolic target volume on ^{18}F-flurodeoxyglucose (FDG) positron emission tomography (PET) images, tumor's intrinsic radio-sensitivity, re-population and hypoxia [3]. Biomarkers that can demonstrate these intrinsic tumor characteristics and how they change with therapy are therefore necessary to stratify potentially non-responding tumors early in the treatment.

Positron Emission Tomography/ Computed Tomography (PET/CT) has been evaluated for RT response assessment [4], [5]. The lower soft-tissue contrast of CT, however, makes the study of anatomical changes inside the tumor sub-volumes difficult. In addition, large inter-observer variability is reported in delineating head and neck tumors on CT images [6].

This paper evaluates the new integrated positron emission tomography/ magnetic resonance (PET/MR) imaging modality for tumor response assessment to radiotherapy. FDG-PET has been tested in the context of RT response assessment and is known to be a useful marker for radio-resistance [4], [5]. The head and neck region is very complex with structures like salivary glands, lymphoid tissue and laryngeal muscle. Higher soft tissue contrast and lower susceptibility to dental filling artifacts makes magnetic resonance imaging (MRI) an appropriate imaging modality in this case [7], [8], [9]. Integration of PET and MR imaging is expected to increase the accuracy of lesion-based analysis resulting from better alignment and synergistic analysis of both imaging data in a region like head and neck that has high mobility and anatomical complexity. Some studies have assessed PET/MR for initial staging of head and neck cancer [10], [11]. PET/MR for RT response assessment, to the best of our knowledge, has not been reported. In this prospective pilot study, we examine on-treatment changes in FDG-PET/MR parameters and show that total lesion glycolysis assessed as early as two weeks into radiotherapy could potentially be used as a biomarker for early response assessment.

II. Materials and Methods

A. Patients

This prospective pilot study was approved by the Domain Specific Review Board and all patients gave written informed consent. Seven patients (4 men, 3 women) with histologically confirmed carcinoma of the head and neck region and planned radical RT (with/ without concurrent chemotherapy) were

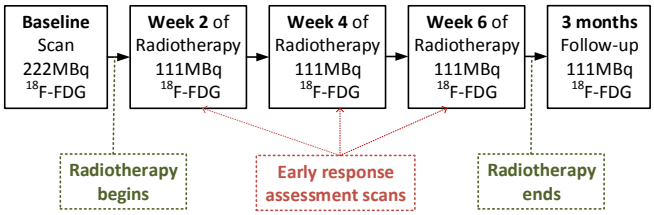

Fig. 1: Multi-point serial scanning schedule.

enrolled in this study. The patients were aged between 36 and 71 years (median age 46 years). Five out of the seven patients had undifferentiated carcinoma at the nasopharynx. One patient had squamous cell carcinoma in the larynx and one had squamous cell carcinoma at the floor of the mouth. All patients received a radiation dose of 70 Gy in 33 fractions over 6.5 weeks.

B. Imaging Schedule

Five multi-parametric PET/MRI scans including dynamic contrast enhanced magnetic resonance imaging (DCE-MRI) and diffusion weighted imaging (DWI) were scheduled per patient. The first scan was obtained at baseline before treatment; subsequent scans were at weeks two, four and six of the RT and the last scan was at three months post-treatment. 222 Megabecquerel (MBq) of FDG was injected on the initial scan and 111 MBq was injected for the subsequent scans. Fig. 1 illustrates the scan schedule.

C. Image Acquisition

Images were acquired on a 3T Biograph mMR (Siemens Healthcare, Germany). All patients fasted for at least six hours prior to examination. The following sequences were acquired using a dedicated head/neck coil; three-dimensional (3D) T1-weighted spin echo image (TR= 736 ms, TE= 8.4 ms), 3D T2-weighted image (TR= 7550 ms, TE= 85 ms), RESOLVE diffusion-weighted (DW) images (b= 0, 100, 500 and 1000 s/mm^2, TR= 8100 ms, TE= 69 ms, acquired voxel size $= 2 \times 2 \times 4$ mm), spoiled gradient echo dynamic contrast enhanced scan (TR= 3.65 ms, TE= 1.23 ms, flip angle $= 15°$, 2.13 s temporal resolution, acquired voxel size $= 0.6 \times 0.6 \times 1$ mm). After ten measurements of the 3D spoiled gradient echo sequence, 0.1 mmol/kg of gadolinium-based contrast agent Gadovist (Bayer, Germany) was intravenously injected at 3 ml/s with a power injector followed by a 20 ml saline flush.

PET images were acquired for 10 minutes in the head and neck region at 60 ± 12 minutes post FDG injection. The images were reconstructed using the iterative ordered-subset expectation maximization algorithm, three iterations and 21 subsets, a Gaussian filter with 3.0 mm full width at half maximum and a 344×344 image matrix. Automatic attenuation correction was performed based on a four-compartment-model attenuation map.

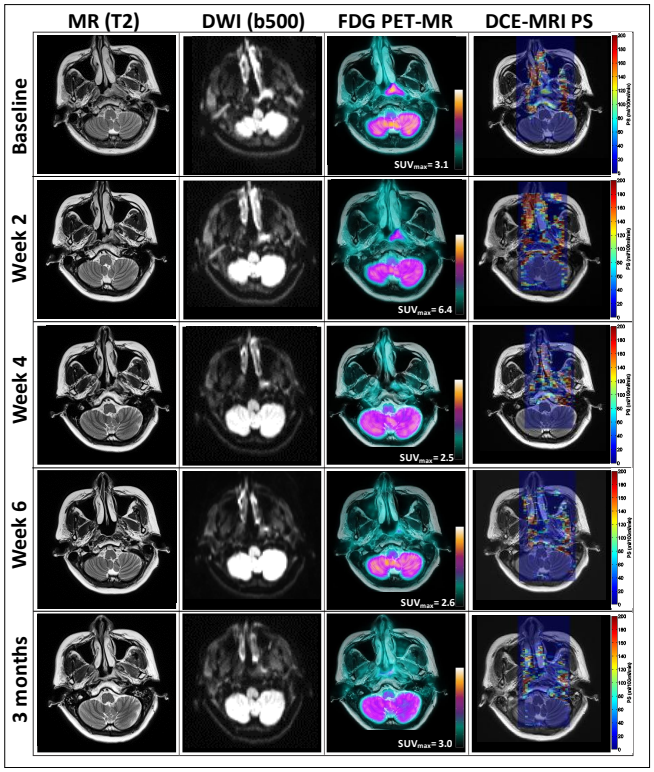

Fig. 2: This figure illustrates multi-modality imaging changes during RT in a patient with complete response (patient 4). Changes in T2-weighted images, DW b500 images, fused PET/MR images and permeability surface-area product (PS) maps are shown.

D. Parameter Analysis

The tumor lesions were manually contoured on T2-weighted MR images and DW images with diffusion coefficient 500 (b = 500) by a senior head and neck cancer radiation oncologist. T2-weighted images were used as anatomic reference for marking the area with restricted diffusion on b500 images. Gross tumor volumes were computed from MR (GTV-MR) and DW (GTV-DW) contours. DW contours were applied to the corresponding apparent diffusion coefficient (ADC) maps and the mean ADC values were computed.

DCE-MRI concentration time curves were analyzed using the distributed parameter (DP) tracer kinetic model [12]. For the arterial input function, a region of interest (ROI) was manually drawn at a vertebral artery. Model fitting was performed by using a nonlinear optimization algorithm, lsqcurvefit in MATLAB R2016a. Pixels with fitting failure were determined by low fraction of modeling information with a threshold of 0.995 or very low SNR and were excluded [13]. DP model provides perfusion (F), permeability surface area product (PS), fractional plasma volume (v_p), fractional extravascular extracellular space volume (v_e), and blood volume transfer constant K^{trans}. The K^{trans} obtained with DP model is a product of first pass extraction ratio (E).

An ROI was drawn enclosing the primary tumor on the standardized uptake value (SUV) image. Maximum standardized

TABLE I: Median[range] changes in various parameters between baseline and weeks 2 and 4 of RT. The numbers in bold are statistically significant with $p < 0.05$.

Parameter	Baseline to week 2	Baseline to week 4
GTV-MR	$\mathbf{-4.32}$	$\mathbf{-8.06}$
(cm^3)	$[\mathbf{-12.19}, \mathbf{-1.30}]$	$[\mathbf{-24.40}, \mathbf{-3.68}]$
GTV-DW	$\mathbf{-4.97}$	$\mathbf{-11.75}$
(cm^3)	$[\mathbf{-15.28}, \mathbf{0.79}]$	$[\mathbf{-19.70}, \mathbf{-1.25}]$
MTV	-0.62	-0.61
(cm^3)	$[-1.32, 0.53]$	$[-3.17, 4.10]$
ADC_{mean}	$\mathbf{0.26}$	$\mathbf{0.34}$
($\times 10^{-3}$ mm^2/s)	$[\mathbf{0.05}, \mathbf{0.48}]$	$[\mathbf{0.08}, \mathbf{0.51}]$
SUV_{mean}	0.91	-1.54
	$[-13.18, 6.33]$	$[-15.20, 0.00]$
SUV_{max}	1.11	-1.87
	$[-15.86, 8.06]$	$[-18.58, 0.08]$
TLG	-1.91	-4.49
($cm^3 \times$ SUV)	$[-28.85, 41.98]$	$[-30.33, 21.68]$
PS	19.36	56.54
(ml/min/100 ml)	$[-65.60, 217.45]$	$[-8.00, 114.07]$

uptake value (SUV_{max}) was computed inside the ROI. A 70% of SUV_{max} threshold was applied to segment out the metabolic target volume (MTV) of the tumor. Minimum, maximum, and mean SUV values were computed inside the MTV. Total lesion glycolysis (TLG) was computed using the product of SUV_{mean} and MTV.

TABLE II: Median[range] changes in various parameters between baseline and week 6 of RT and between baseline and three months post-treatment follow-up. The numbers in bold are statistically significant with $p < 0.05$.

Parameter	Baseline to week 6	Baseline to 3 months
GTV-MR	$\mathbf{-12.78}$	$\mathbf{-10.97}$
(cm^3)	$[\mathbf{-28.11}, \mathbf{-4.37}]$	$[\mathbf{-26.72}, \mathbf{-3.24}]$
GTV-DW	$\mathbf{-14.99}$	$\mathbf{-12.90}$
(cm^3)	$[\mathbf{-15.98}, \mathbf{-5.97}]$	$[\mathbf{-30.27}, \mathbf{-5.71}]$
MTV	-0.51	$\mathbf{-1.53}$
(cm^3)	$[-2.98, 1.29]$	$[\mathbf{-4.10}, \mathbf{-0.71}]$
ADC_{mean}	$\mathbf{0.53}$	$\mathbf{0.42}$
($\times 10^{-3}$ mm^2/s)	$[\mathbf{0.47}, \mathbf{0.61}]$	$[\mathbf{-0.08}, \mathbf{0.74}]$
SUV_{mean}	-2.32	-1.42
	$[-14.55, -0.38]$	$[-4.68, 1.39]$
SUV_{max}	-2.81	-1.91
	$[-17.87, -0.50]$	$[-5.40, 1.29]$
TLG	$\mathbf{-4.31}$	-10.86
($cm^3 \times$ SUV)	$[\mathbf{-30.78}, \mathbf{4.67}]$	$[-32.42, -2.58]$
PS	-24.55	-15.00
(ml/min/100 ml)	$[-32.05, -17.04]$	$[-18.24, 36.50]$

III. Results

Seven patients have been scanned in this study. Four patients have completed all five scans. Three patients missed some mid-treatment scans due to treatment related side-effects, namely fatigue and mucositis. All patients attained complete radiological response at three months post-treatment and to date, there is one loco-regional recurrence (patient 3). One patient died of distant metastasis to the liver (patient 2). Fig. 2 illustrates multi-parametric changes in the tumor for a representative patient with complete response (patient 4).

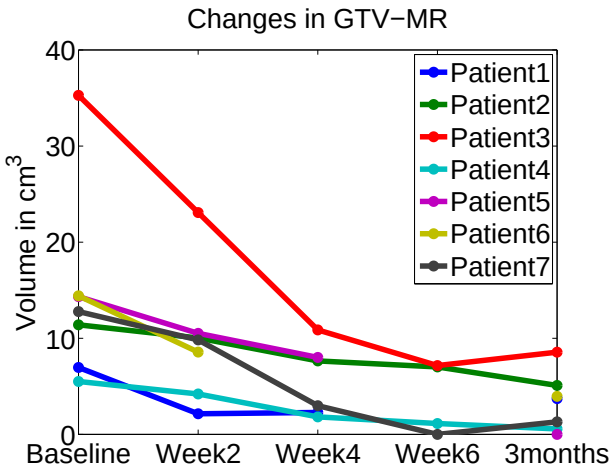

(a)

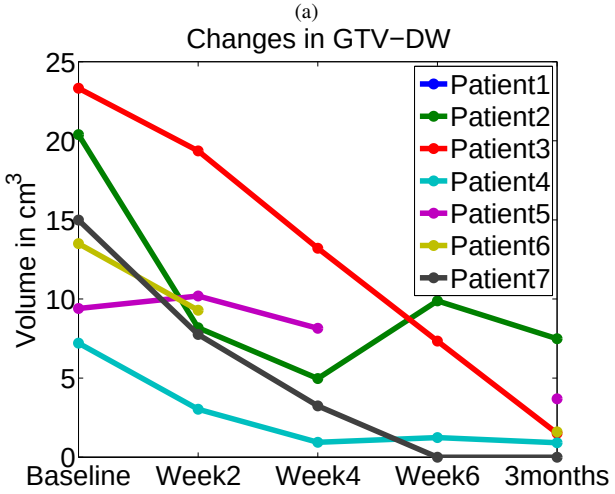

(b)

Fig. 3: Changes in (a) GTV-MR and (b) GTV-DW for the seven patients. Progressive reductions were observed both in GTV-MR and GTV-DW as RT commenced.

The anatomic tumor volume delineated on MR and DW images reduced as RT commenced (Fig. 3). Tables I and II enlist changes in various parameters between baseline and the subsequent scans. The numbers in bold represent statistically significant observations with $p < 0.05$. Statistically significant reductions were observed in GTV-MR and GTV-DW at all imaging time-points with respect to the baseline measurement. An average of 50% reduction in GTV-MR and GTV-DW is observed between baseline and week 4 scan.

Statistically significant rise in mean ADC was observed at all imaging time-points with respect to the baseline observation (Tables I and II). The mean ADC value in patient 3 was, however, below baseline at three months follow-up scan (Fig. 4(a)). Patient 3 was diagnosed with loco-regional recurrence eight months after the last follow-up scan.

A decreasing trend was observed in MTV for majority of the patients. Fig. 4(b) shows the variations in MTV in all the patients. The patient with loco-regional recurrence (patient 3) exhibited increase in MTV at week 2 of RT with a subsequent decrease. Residual MTV at three months follow-up scan in

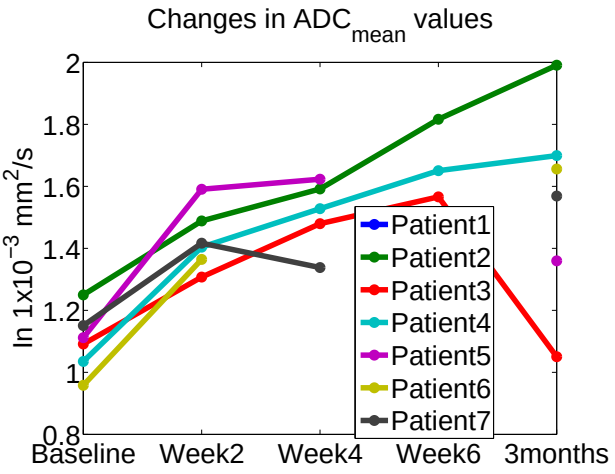

(a)

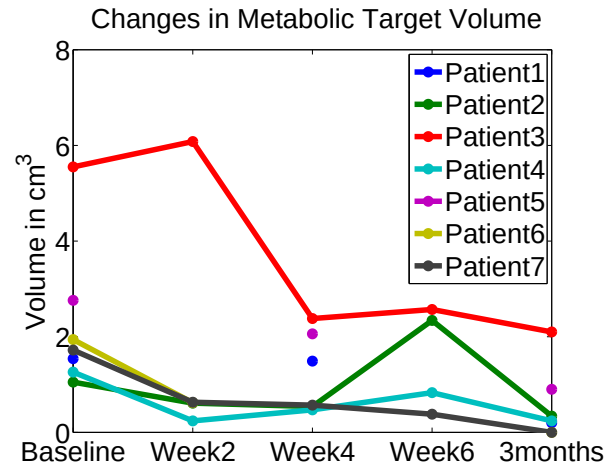

(b)

Fig. 4: Changes in (a) mean ADC values and (b) MTV for the seven patients. Mean ADC values increased with treatment. Patient with recurrence showed a drop in mean ADC at three months post-treatment scan. There was a mid-treatment increase in MTV in three out of the seven patients.

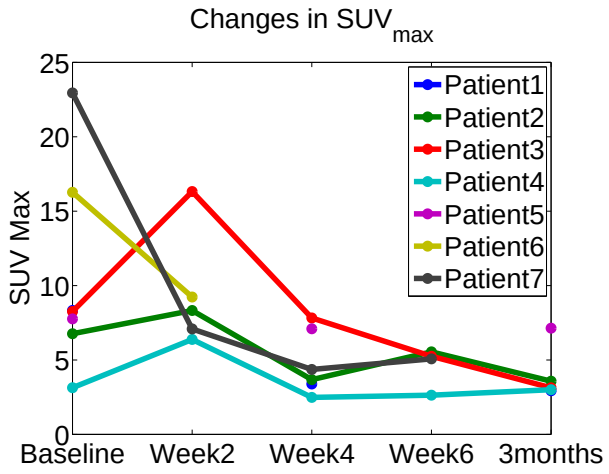

(a)

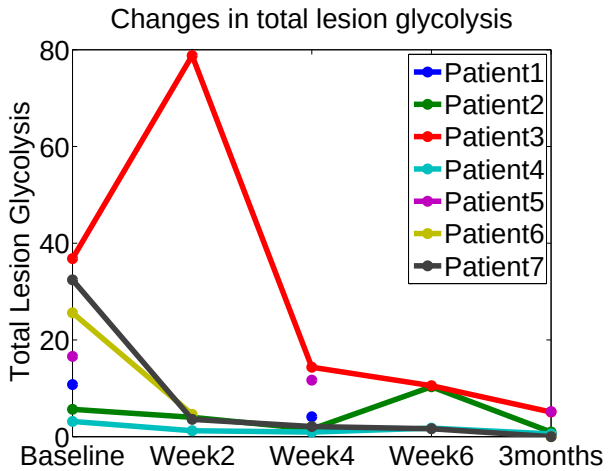

(b)

Fig. 5: Changes in (a) $\mathrm{SUV}_{\max}$ and (b) TLG for all patients. Mid-treatment rise in $\mathrm{SUV}_{\max}$ was observed in four out of the seven patients. Patient 3 had a big TLG peak at week 2 of radiotherapy.

patient 3 was also higher than that observed in all other patients. The missing points in the graph correspond to the missed scans.

In three out of the seven patients, a temporary rise in $\mathrm{SUV}_{\max}$ was observed at week 2 of RT. Majority of patients demonstrated a mid-treatment rise in $\mathrm{SUV}_{\max}$ at some point during the therapy (Fig. 5(a)). Statistically significant changes in mean or maximum SUV were not observed for any imaging time-point (Tables I and II). TLG was found to steadily decrease with treatment except for patients 2 and 3 who had temporary increase in TLG at weeks 6 and 2 respectively (Fig. 5(b)). Statistically significant reduction in TLG was observed between observations at baseline and week 6 (Table. II).

No consistent trends were observed in the functional parameters extracted from DCE-MRI. Permeability surface area product was found to temporarily increase between baseline and week 4 of treatment with a subsequent decrease to below baseline by week 6 and three months follow-up scans (Tables. I and II).

IV. Discussion

The therapeutic index of RT with or without chemotherapy is low. The ability to stratify patients as early as possible can potentially improve overall cancer outcome for this group of patients by selectively targeting more aggressive tumors for more intensive treatment. The integrated PET/MR imaging offers the opportunity to mine multiple anatomical and functional parameters from the tumor sub-volumes during treatment. This paper presents analysis of how various imaging parameters change inside the tumor sub-volume as the therapy progresses.

Anatomic volume on T2−weighted images, GTV-MR, was reduced by $> 30\%$ at week 2 and by $> 50\%$ at week 4. Similar percentage changes in anatomical volumes were reported by other studies investigating changes in tumor volume within

treatment in head and neck cancer cases [5], [14], [15]. These consistent findings across multiple centers validate the feasibility of tumor-based early response assessment.

Volume contoured on DWI b500 images also reduce significantly with treatment. This finding is similar to previously reported changes in volumes based on DWI images [14]. Significant increase in mean ADC values is observed at all imaging time-points (Tables I and II). Increase in diffusion is correlated with reduced tumor cellularity and likely response to treatment [5]. Multiple studies on DWI as a predictor of tumor response validate this hypothesis and report similar results [14], [16], [17], [18]. The decrease in ADC value for patient 3 at three months follow-up scan could be indicative of tumor cell re-population.

The changes in MTV were found to be inconsistent. In three out of the seven patients, there was an increase in MTV at some point in the treatment. This increase could be related to inflammation in the mucosa surrounding the tumor. The maximum SUV uptake also peaked at week 2 for three out of the seven patients, potentially due to similar reasons. The patient with recurrence (patient 3), however, demonstrated much higher increase in $\mathrm{SUV}_{\max}$ at week 2.

Total lesion glycolysis is increasingly being studied in the context of response assessment [19], [20], [21], [22]. TLG was found to decrease with treatment with two exceptions, patient 2 and patient 3. Patient 3 had a big TLG peak at week 2 and patient 2 had a TLG peak at week 6. The TLG peak of patient 3, at week 2 could potentially be due to tumor hypoxia, RT-induced re-population or inflammation.

Parameters from DCE-MRI have been shown to correlate with microvascular density and hypoxia, as well as RT outcome [24], [25], [26]. Role of these parameters, however, is unclear in mid-therapy assessment. We did not observe coherent trends in the DCE parameters. Temporary increase in permeability surface area product observed between baseline and at weeks 2 and 4 may suggest vessel damage due to treatment.

Our analysis on the first few subjects suggest that significant changes can be observed in various anatomical and functional parameters as early as week 2 of treatment. ADC and TLG, in combination with other anatomical parameters could potentially be bio-markers for treatment response assessment. Relative changes in these parameters could be more useful indicators than their absolute values. Further investigation on a larger patient group is required to confirm these findings. This study is limited by its small data size. We are expanding the patient cohort to further confirm these early findings. Another possible source of inaccuracy could be the manual contouring of the tumor in the DW images. The geometric distortions inherent in the standard EPI sequence DW images make tumor contouring very difficult and preclude the use of DW images in radiotherapy planning [27]. To mitigate this source of inaccuracy we have used the RESOVLE sequence from Siemens Healthcare, Germany. RESOLVE generates images with less distortion and higher spatial resolution.

V. Conclusion

The clinical goal behind the presented research is to find imaging bio-markers that can reliably differentiate responders from potential non-responders early in the treatment. This prospective pilot study evaluates the optimal timing and utility of interim functional imaging with serial FDG PET/MRI scans before, during and after radiotherapy. Preliminary data suggests that an interim scan at week 2 of RT has the potential to be a clinically feasible time-point for response assessment. Functional parameters derived from PET and diffusion weighted imaging, in combination with other parameters, are potentially useful imaging markers for treatment response and disease outcome. Decreasing total lesion glycolysis and increasing apparent diffusion coefficient seem to be indicative of good treatment response. Further analysis on a bigger patient group is necessary to confirm these findings.

References

[1] A. A. Forastiere, H. Goepfert, M. Maor, T. F. Pajak, R. Weber, W. Morrison, B. Glisson, A. Trotti, J. A. Ridge, C. Chao, G. Peters, D.-J. Lee, A. Leaf, J. Ensley, and J. Cooper, "Concurrent chemotherapy and radiotherapy for organ preservation in advanced laryngeal cancer," *N Engl J Med.*, vol. 349, no. 22, pp. 2091-2098, 2003.

[2] J. T. Johnson, "A surgeon looks at cervical lymph nodes," *Radiology*, vol. 175, pp. 607-610, 1990.

[3] A. C. Begg, "Predicting recurrence after radiotherapy in head and neck cancer," *Semin Radiat Oncol.*, vol. 22, no. 2, pp. 108-118, 2012.

[4] M. Hentschel, S. Appold, A. Schreiber, A, Abramyuk, N. Abolmaali, J. Kotzerke, M. Baumann, and K. Zphel, "Serial FDG-PET on patients with head and neck cancer: implications for radiation therapy," *Int J Radiat Biol.*, vol. 85, pp. 796-804, 2009.

[5] M. Subesinghe, A. F. Scarsbrook, S. Sourborn, D. J. Wilson, G. McDermott, R. Speight, N. Roberts, B. Carey, R. Forrester, S. V. Gopal, J. R. Sykes, and R. J. D. Prestwich, "Alterations in anatomic and functional imaging parameters with repeated FDG PET-CT and MRI during radiotherapy for head and neck cancer: a pilot study, *BMC Cancer*, vol. 15, no. 137, 2015.

[6] J. S. Cooper, S. K. Mukherjee, A. Y. Toledano, C. Beldon, I. M. Schmalfuss, R. Amdur, S. Sailer, L. A. Loevner, P. Kousouboris, K. K. Ang, J. Cormack, and J. Sicks, "An evaluation of the variability of tumor-shape definition derived by experienced observers from CT images of supraglottic carcinomas (ACRIN protocol 6658)," *Int J Radiat Oncol Biol Phys.*, vol. 67, no. 4, pp. 924-930, 2007.

[7] T. Beyer, L. S. Freudenberg, J. Czernin, and D. W. Townsend, "The future of hybrid imaging-part 3: PET/MR, small-animal imaging and beyond," *Insights Imaging*, vol. 2, pp. 235-246, 2011.

[8] G. Antoch and A. Bockisch, "Combined PET/MRI: a new dimension in whole-body oncology imaging?," *Eur J Nucl Med Mod Imaging*, vol. 36 Suppl 1, pp. 113-120, 2009.

[9] T. Klinke, A. Daboul, J. Maron, T. Gredes, R. Puls, A. Jaghsi, and R. Biffar, "Artifacts in magnetic resonance imaging and computed tomography caused by dental materials," *PLoS One*, vol. 7, pp. e31766, 2012.

[10] S. J. Lee, H. J. Seo, G. J. Cheon, J. H. Kim, E. E. Kim, K. W. Kang, J. C. Paeng, J.-K. Chung, and D. S. Lee, "Usefulness of integrated PET/MRI in head and neck cancer: a preliminary study," *Nucl Med Mol Imaging*, vol. 48, pp. 98-105, pp. 98-105, 2014.

[11] I. Platzek, B. B.-Baumann, M. Schneider, V. Gudziol, J. Langner, G. Schramm, M. Laniado, J. Kotzerke, and J. Hoff, "PET/MRI in head and neck cancer: initial experience," *Eur J Nucl Med Mol Imaging*, vol 40, pp. 6-11, 2013.

[12] T. S. Koh, L. H. Cheong, Z. Hou, and Y. C. Soh, "A physiologic model of capillary-tissue exchange for dynamic contrast-enhanced imaging of tumor microcirculation," *IEEE Trans. Bio Med. Eng.*, vol. 50, no. 2, pp. 2159-2167, 2003.

[13] D. Balvay, F. Frouin, G. Calmon, B. Bessoud, E. Kahn, N. Siauve, O. Clement, and C. A. Cuenod, "New criteria for assessing fit quality in dynamic contrast-enhanced T1-weighted MRI for perfusion and permeability imaging," *Magn. Reson. Med.*, vol. 54, pp. 868-877, 2005.

[14] P. Dirix, V. Vandecaveye, F. De Keyzer, S. Stroobants, R. Hermans, and S. Nuyts, "Dose painting in radiotherapy for head and neck squamous cell carcinoma: value of repeated functional imaging with 18F-FDG PET, 18F-fluoromisonidazole PET, diffusion-weighted MRI, and dynamic contrast-enhanced MRI, *J Nucl Med*, vol. 50, pp. 1020-1027, 2009.

[15] Y. Cao, A. Popovtzer, D. Li, D. B. Chepeha, J. S. Moyer, M. E. Prince, F. Worden, T. Teknos, C. Bradford, S. K. Mukherji, and A. Eisbruch, "Early prediction of outcome in advanced head-and-neck cancer based on tumor blood volume alterations during therapy: a prospective study," *Int J Radiat Oncol Biol Phys.*, vol. 72, no. 5, pp. 1287-90, 2008.

[16] V. Vandecaveye, P. Dirix, F. De Keyzer, K. O. de Beeck, V. V. Poorten, I. Roebben, S. Nuyts, and R. Hermans, "Predictive value of diffusion-weighted magnetic resonance imaging during chemoradiotherapy for head and neck squamous cell carcinoma," *Eur Radiol.*, vol. 20, no. 7, pp. 1703-1714, 2010.

[17] S. Kim, L. Loevner, H. Quon, E. Sherman, G. Weinstein, A. Kilger, and H. Poptani, "Diffusion-weighted magnetic resonance imaging for predicting and detecting early response to chemoradiation therapy of squamous cell carcinomas of the head and neck," *Clin Cancer Res.*, vol 15, no. 3. pp. 986-994, 2009.

[18] M. Hatakenaka, K. Nakamura, H. Yabuuchi, Y. Shioyama, Y. Matsuo, K. Ohnishi, S. Sunami, T. Kamitani, T. Setoguchi, T. Yoshiura, T. Nakashima, K. Nishikawa, and H. Honda, "Pretreatment apparent diffusion coefficient of the pirmary lesion correlates with local failure in head-and-neck cancer treated with chemoradiotherapy or radiotherapy," *Int J Radiat Oncol Biol Phys.*, vol. 81, no. 2, pp. 339-345, 2010.

[19] S. M. Larson, Y. Erdi, T. Akhurst, M. Mazumdar, H. A. Macapinlac, R. D. Finn, C. Casilla, M. Fazzari, N. Srivastava, H. W. D. Yeung, J. L. Humm, J. Guillem, R. Downey, M. Karpeh, A. E. Cohen, and R. Ginsberg, "Tumor treatment response based on visual and quantitative changes in global tumor glycolysis using PET-GDG imaging: the visual response score and the change in total lesion glycolysis," *Clin Positron Imaging*, vol. 2, no. 3, pp. 159-171, 1999.

[20] J. G. Guillem, H. G. Moore, T. Akhurst, D. S. Klimstra, L. Ruo, M. Mazumdar, B. D. Minsky, L. Saltz, W. D. Wong, and S. Larson, "Sequential preoperative fluorodeoxyglucose-positron emission tomography assessment of response to pre-operative chemoradiation: a means for determining long-term outcomes of rectal cancer," *J Am Coll Surg.*, vol. 199, no. 1, pp. 1-7, 2004.

[21] R. J. Francis, M. J. Byrne, A. A. van der Schaff, J. A. Boucek, A. K. Nowak, M. Phillips, R. Price, A. P. Patrikeos, A. W. Musk, and M. J. Millward, "Early prediction of response to chemotherapy and survival in malignant pleural mesothelioma using a novel semiautomated 3-dimensional volume-based analysis of serial 18F-FDG PET scans," *J Nucl Med.*, vol. 48, no. 9, pp. 1449-58, 2007.

[22] F. Hofheinz, A. Lougovski, K. Zophel, M. Hentschel, I. G. Steffen, I. Apostolova, F. Wedel, R. Buchert, M. Baumann, W. Brenner, J. Kotzerke, and J. van den Hoff, "Increased evidence for the prognostic value of primary tumor asphericity in pretherapeutic FDG PET for risk stratification in patients with head and neck cancer," *Eur J Nucl Med Mol Imaging*, vol. 42, pp. 429-437, 2015.

[23] M. Hentschel, S. Appold, A. Schreiber, N. Abolmaali, A. Abramyuk, W. Drr, J. Kotzerke, M. Baumann, and K. Zphel, "Early FDG PET at 10 or 20 Gy under chemoradiotherapy is prognostic for locoregional control and overall survival in patients with head and neck cancer," *Eur J Nucl Med Mol Imaging*, vol. 38, no. 7, pp. 1203-1200, 2011.

[24] P. J. Hoskin, M. I. Saunders, K. Goodchild, M. E. Powell, N. J. Taylor, and H. Baddeley, "Dynamic contrast enhanced magnetic resonance scanning as a predictor of response to accelerated radiotherapy for advanced head and neck cancer," *Br J Radiol.*, vol. 72, pp. 1093-1098, 1999.

[25] J. F. Jansen, H. Schoder, N. Y. Lee, H. E. Stambuk, Y. Wang, M. G. Fury, S. G. Patel, D. G. Pfister, J. P. Shah, J. A. Koutcher, and A. Shukla-Dave, "Tumor metabolism and perfusion in head and neck squamous cell carcinoma: pretreatment multimodality imaging with ^{1}H magnetic resonance spectroscopy, dynamic contrast-enhanced MRI, and [^{18}F]FDG-PET," *Int J Radiat Oncol Biol Phys.*, vol. 82, no. 1, pp. 299-307, 2012.

[26] M. A. Zahra, K. G. Hollingsworth, E. Sala, D. J. Lomas, and L. T. Tan, "Dynamic contrast-enhanced MRI as a predictor of tumor response to radiotherapy," *Lancet Oncol.*, vol. 8, no. 1, pp. 63-74, 2007.

[27] T. Schakel, J. M. Hoogduin, C. H. J. Terhaard, and M. E. P. Philippens, "Diffusion weighted MRI in head-and-neck cancer: geometrical accuracy," *Radiother Oncol*, vol. 109, no. 3, pp. 394-397, 2013.